J|A|C|S
ARTICLES
Published on Web 03/24/2006

Theoretical Study on Tertiary Structural Elements of β-peptides: Nanotubes Formed from Parallel-Sheet-Derived Assemblies of β-Peptides

Tamás Beke,[†] Imre G. Csizmadia,[‡] and András Perczel*,[†]

Contribution from the Department of Organic Chemistry, Eötvös University, P.O. Box 32, H-1518 Budapest 112, Hungary, and Department of Chemistry and Chemical Informatics, Faculty of Education, University of Szeged, Szeged, H-6725, Hungary

Received December 15, 2005; E-mail: perczel@para.chem.elte.hu

Abstract: Parallel or polar strands of β-peptides spontaneously form nanotubes of different sizes in a vacuum as determined by ab initio calculations. Stability and conformational features of $[CH_3CO-(\beta\text{-Ala})_k-NHCH_3]_l$ ($1 \le k \le 4$, $2 \le l \le 4$) models were computed at different levels of theory (e.g., B3LYP/6-311++G(d,p)//B3LYP/6-31G(d), with consideration of BSSE). For the first time, calculations demonstrate that sheets of β-peptides display nanotubular characteristics rather than two-dimensional extended β-layers, as is the case of α-peptides. Of the configurations studied, $k = l = 4$ gave the most stable nanotubular structure, but larger assemblies are expected to produce even more stable nanotubes. As with other nanosystems such as cyclodextrane, these nanotubes can also incorporate small molecules, creating a diverse range of applications for these flexible, biocompatible, and highly stable molecules. The various side chains of β-peptides can make these nanosystems rather versatile. Energetic and structural features of these tubular model systems are detailed in this paper. It is hoped that the results presented in this paper will stimulate experimental research in the field of nanostructure technology involving β-peptides.

Introduction

One of the most stable conformers of α-L-amino acid residues is the extended-like or β_L-type backbone orientation.[1] Such elongated structures can be observed when multiple adjacent amino acid residues consecutively adopt $\varphi \approx -150°$ and $\psi \approx 150°$ values or $(\beta_L)_n$ for short (Scheme 1).[2] Such β-strands are able to assemble further into two (or multiple) stranded β-pleated sheets that can either have parallel or antiparallel relative spatial arrangement.[3−6] A large number of globular proteins contain complex β-pleated sheet networks.[7−9] However, there are two well-known extremes in proteins composed primarily of multiple β-strands, silk[10] and twisted β-barrel proteins.[11−14] In the first case, the overall structure resembles a multilayer plate, whereas strands assemble in a circular fashion in the β-barrel, forming a tubular or barrel supramolecular structure.

Similar to α-peptides, β-peptides can also adopt an extended-like conformation. As shown by experimental data[15−23] and theoretical studies,[24,25] the slightly spiral S_{PM} (or U4) conformational building unit[26,27] ($\varphi \approx -70°$, $\mu \approx 170°$, $\psi \approx 180°$)

† Eötvös University.
‡ University of Szeged.

(1) Perczel, A.; Angyan, J. G.; Kajtar, M.; Viviani, W.; Rivail, J. L.; Marcoccia, J. F.; Csizmadia, I. G. *Journal of the American Chemical Society* **1991**, *113*, 6256−6265.
(2) Berg, J.; Tymoczko, J.; Stryer, L. *Biochemistry*, 5th ed.; W.H. Freeman: New York, 2002.
(3) Salemme, F. R. *Progress in Biophysics & Molecular Biology* **1983**, *42*, 95−133.
(4) Shamovsky, I. L.; Ross, G. M.; Riopelle, R. J. *Journal of Physical Chemistry B* **2000**, *104*, 11296−11307.
(5) Petsko, G. A.; Ringe, D. *Protein Structure and Function*; Nes Science Press Ltd: London, 2004.
(6) Perczel, A.; Gaspari, Z.; Csizmadia, I. G. *Journal of Computational Chemistry* **2005**, *26*, 1155−1168.
(7) Hester, G.; Wright, C. S. *Journal of Molecular Biology* **1996**, *262*, 516−531.
(8) Frank, M. K.; Dyda, F.; Dobrodumov, A.; Gronenborn, A. M. *Nature Structural Biology* **2002**, *9*, 877−885.
(9) Ye, S.; Goldsmith, E. J. *Current Opinion in Structural Biology* **2001**, *11*, 740−745.
(10) Tirrell, D. A. *Science* **1996**, *271*, 39−40.
(11) Bolter, B.; Soll, J. *EMBO Journal* **2001**, *20*, 935−940.
(12) Kleinschmidt, J. H. *Cellular and Molecular Life Sciences* **2003**, *60*, 1527−1528.
(13) Karplus, P. A.; Daniels, M. J.; Herriott, J. R. *Science* **1991**, *251*, 60−66.
(14) Locher, K. P.; Rees, B.; Koebnik, R.; Mitschler, A.; Moulinier, L.; Rosenbusch, J. P.; Moras, D. *Cell* **1998**, *95*, 771−778.
(15) Martinek, T. A.; Toth, G. K.; Vass, E.; Hollosi, M.; Fulop, F. *Angewandte Chemie, International Edition* **2002**, *41*, 1718−1721.
(16) Seebach, D.; Overhand, M.; Kuhnle, F. N. M.; Martinoni, B.; Oberer, L.; Hommel, U.; Widmer, H. *Helvetica Chimica Acta* **1996**, *79*, 913−941.
(17) Seebach, D.; Abele, S.; Gademann, K.; Jaun, B. *Angewandte Chemie, International Edition* **1999**, *38*, 1595−1597.
(18) Krauthauser, S.; Christianson, L. A.; Powell, D. R.; Gellman, S. H. *Journal of the American Chemical Society* **1997**, *119*, 11719−11720.
(19) Karle, I.; Gopi, H. N.; Balaram, P. *Proceedings of the National Academy of Sciences of the United States of America* **2002**, *99*, 5160−5164.
(20) Chung, Y. J.; Huck, B. R.; Christianson, L. A.; Stanger, H. E.; Krauthauser, S.; Powell, D. R.; Gellman, S. H. *Journal of the American Chemical Society* **2000**, *122*, 3995−4004.
(21) Diederichsen, U.; Schmitt, H. W. *European Journal of Organic Chemistry* **1998**, 827−835.
(22) Chung, Y. J.; Christianson, L. A.; Stanger, H. E.; Powell, D. R.; Gellman, S. H. *Journal of the American Chemical Society* **1998**, *120*, 10555−10556.
(23) Daura, X.; Gademann, K.; Schafer, H.; Jaun, B.; Seebach, D.; van Gunsteren, W. F. *Journal of the American Chemical Society* **2001**, *123*, 2393−2404.
(24) Gunther, R.; Hofmann, H. J.; Kuczera, K. *Journal of Physical Chemistry B* **2001**, *105*, 5559−5567.
(25) Beke, T.; Somlai, C.; Perczel, A. *Journal of Computational Chemistry* **2006** *27*, 20−38.

10.1021/ja0585127 CCC: $33.50

Scheme 1. Buildup Scheme of Sheetlike Structures of α- and β-Peptides: From Monomers to Different Secondary Structure Elements up to the Formation of Alternative Tertiary Structures

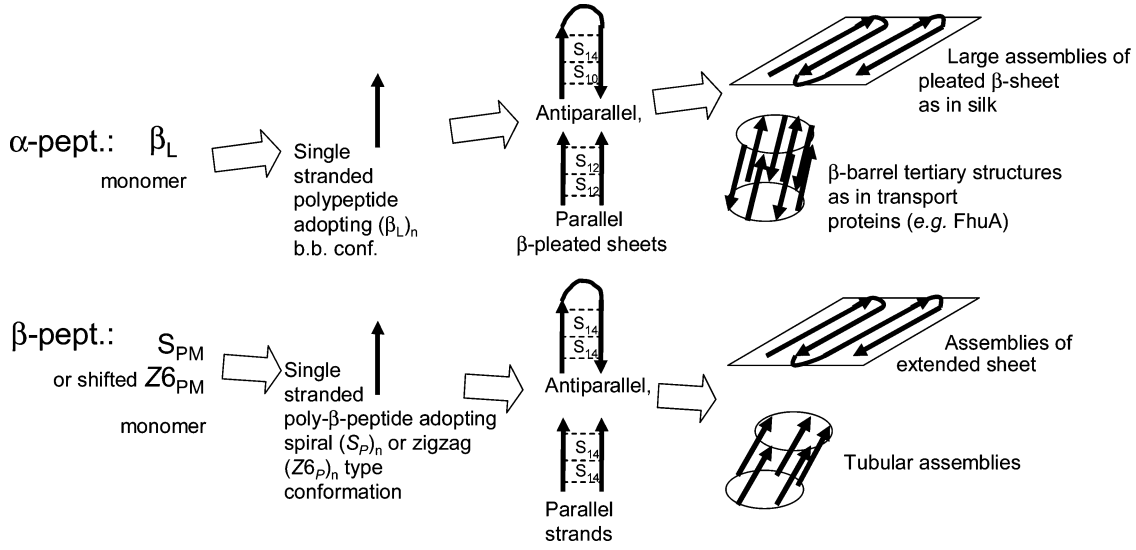

(Figure 1) of a β-amino acid residue can form single β-strand-like structures. In addition, there are already numerous studies revealing both parallel and antiparallel sheet structures.[16−20,23,28,29] However, there is currently no structural evidence for multiple stranded sheets of poly-β-peptides forming either "silk-like" or "β-barrel-like" supramolecular complexes.

Using CD and UV spectrometry, Diederichsen et al.[21] described the presence of β-strand/sheet-like ordering in short, 4−6 residue long β-homoalanyl−PNA complexes. The extended-like structure of β-homoalanine appears in the complex due to the Hoogsteen and Watson−Crick pairing mode of side-chain bases. The *cis*-(1*R*,2*S*-ACPC) pentamer and heptamer models designed by Martinek et al.[15] form a nonpolar β-strand-like structure, which is most likely the shifted prototype of $Z6_P$.[25] This shift appears due to the rigid *cis*-ACPCs, which constrain the torsional angle μ to a gauche position. Two stranded antiparallel sheets are most often formed when connected by a β-hairpin. This latter turn can be constructed using various α- and β-amino acid residues or other derivatives, such as the heterochiral dinipecotic (i.e. two homoproline containing) segment,[20,22] proline[18,19] or β^2-HVal-β^3-HLys[17] sequences. One of the earliest and most promising "spontaneously" self-assembled parallel sheets were constructed by Seebach et al.[16,17] These relatively short β-peptides, namely β^3- and $\beta^{2,3}$-tripeptide esters, form parallel sheets in the crystal lattice.

Other parallel sheets were constructed by Gellman et al.,[28] where the Pro-DADME segment was used to connect sheets. Several of these models were able to form multistranded sheets in the crystal,[16,17,19,28] which, when combined with other studies on the assembling properties of β-peptides,[30,31] showed that β-peptides have the affinity to form higher order assemblies given the appropriate conditions.

On the road of engineering β-proteins and β-enzymes that could eventually maintain their functionality even in a world full of peptidases; the construction of β-peptides with stable tertiary structures would be a landmark step.[32] Initial attempts have resulted in valuable information on how two helices linked by disulfide bond could interact.[33] Other β-peptide models with cyclic side chains were shown to be present in the form of helix bundles in aqueous media.[30,31] Based on spectroscopic evidence, it was suggested that, at higher concentrations, the helical subunits of 3_{14}-helix former β-henicosapeptide[34] can aggregate into a quaternary-like structure. Furthermore, β-peptides adopting helical conformations were used as scaffolds for duplex formations driven by nucleobase pairing.[35−37] Although in the latter supramolecular complex a tertiary structure formation can be monitored, there is no direct interaction between the β-peptide subunits.

It was suggested that helix formation from β-peptides can be prevented by incorporating $\beta^{2,3}$ disubstituted amino acids.[17,23] The enforced linearity of the backbone fold is the basis of the formation of different pleated sheets.[16,17,32] However, no true example of supersecondary structure elements of β-peptides was pinpointed.

A recent theoretical study on sheet structures conducted by Lin et al.[29] laid the groundwork for the investigation of extended-like multiple stranded sheet structures of β-peptides. In the latter study, all conformers forming the large sheet network were partially constrained. As a result, the true three-dimensional (3D) nature of these superstructures was not deciphered, although

(26) Beke, T.; Csizmadia, I. G.; Perczel, A. *Journal of Computational Chemistry* **2004**, *25*, 285−307.
(27) Mohle, K.; Gunther, R.; Thormann, M.; Sewald, N.; Hofmann, H. J. *Biopolymers* **1999**, *50*, 167−184.
(28) Langenhan, J. M.; Guzei, I. A.; Gellman, S. H. *Angewandte Chemie, International Edition* **2003**, *42*, 2402−2405.
(29) Lin, J. Q.; Luo, S. W.; Wu, Y. D. *Journal of Computational Chemistry* **2002**, *23*, 1551−1558.
(30) Raguse, T. L.; Lai, J. R.; LePlae, P. R.; Gellman, S. H. *Organic Letters* **2001**, *3*, 3963−3966.
(31) Hetenyi, A.; Mandity, I. M.; Martinek, T. A.; Toth, G. K.; Fulop, F. *Journal of the American Chemical Society* **2005**, *127*, 547−553.
(32) Seebach, D.; Beck, A. K.; Bierbaum, D. J. *Chemistry and Biodiversity* **2004**, *1*, 1111−1239.
(33) Cheng, R. O.; DeGrado, W. F. *Journal of the American Chemical Society* **2002**, *124*, 11564−11565.
(34) Kimmerlin, T.; Seebach, D.; Hilvert, D. *Helvetica Chimica Acta* **2002**, *85*, 1812−1826.
(35) Chakraborty, P.; Diederichsen, U. *Chemistry−A European Journal* **2005**, *11*, 3207−3216.
(36) Brückner, A. M.; Chakraborty, P.; Gellman, S. H.; Diederichsen, U. *Angewandte Chemie, International Edition*, **2003**, *42*, 4395−4399.
(37) Fülöp, F.; Martinek, T. A.; Tóth, G. K. *Chemical Society Reviews* **2006**, (Advance Article), DOI: 10.1039/b501173f.

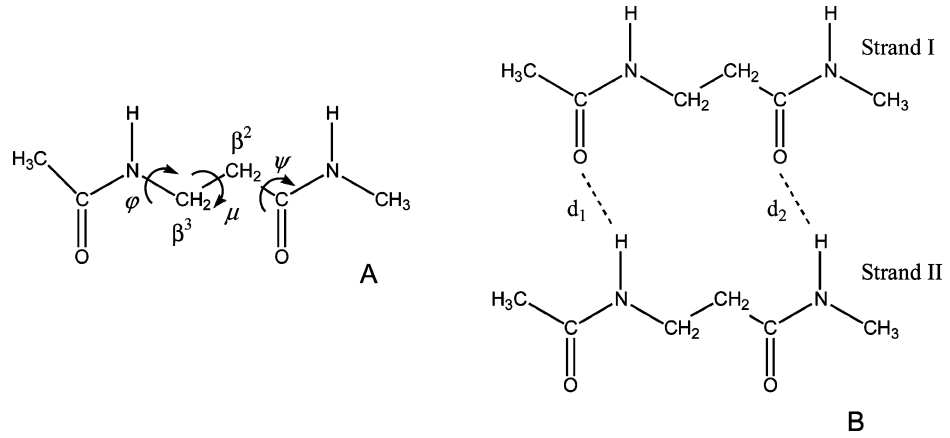

Figure 1. (A) Major conformational variables of a simple β-amino acid diamide, CH_3CO-β-Ala-$NHCH_3$, the structural building unit of sheet assemblies. (B) Two interacting, but noncovalently attached, subunits connected by H-bonds.

they perceptively noted that a larger assembly might have a considerable amount of overall twist based on optimized short models.

In the present paper, we will demonstrate that the foreseen twisting, combined with the experimentally observed tendency that selected β-peptides have the ability to form sheets, appears to such an extent that it "catalyzes" the formation of a tubular network in the gas phase, resulting in nanostructures of varying sizes.

These structures could be regarded as the first example of tertiary structures of β-peptides, showing some similarity with β-barrel assemblies seen in proteins. We have investigated the conformational and energetic properties of multiple stranded extended sheet-derived (or in short sheet) structures formed by simple β-peptides. We will show the molecular details of the self-assembled superstructures and the various forms of tubular systems present in the gas phase.

As highlighted by Jean-Marie Lehn,[38] self-assembling and supramolecular chemistry such as nanochemistry is one of the most promising research areas. Peptide nanotubes are of great importance, and nanotube biotechnology is one of the most rapidly emerging fields of research and development.[39−47] Nanotubes offer diverse applicability as conductors,[48] nanoreactors,[46] or ion channels.[39,49] In the 1990s, cyclic α-peptides[40] and cyclic β-peptides[39] were found to form peptide nanotubes, becoming a leading area of organic nanotechnology.[39,40,46,47] Unlike nanotubes made out of carbon and stabilized by covalent bonds, the 3D assembly of these cyclic peptides is usually stabilized by specific hydrogen bonds and lacks covalent attachment between subunits.[39,40] The various side chains of amino acid residues (e.g., polar, nonpolar, acidic, basic) provide an opportunity to alter and fine-tune the chemical properties of peptide nanotubes, greatly increasing the versatility of these molecules. Furthermore, peptide nanotubes may be regarded as biocompatible substances. However, natural peptides are not resistant to proteolytic enzymes, and their medical application is heavily restricted. In contrast, β-peptides are significantly more stable in vivo, showing no tendency to bind to the active sites of proteolytic enzymes.[50−52] Furthermore, the chemical nature of β-peptides and the presence of two consecutive methylene carbon atoms in the backbone allow the positioning of side chain(s) in many more ways than possible in the case of α-peptides.[53] These features make β-peptides promising agents for novel peptidomimetics.[54−57] As with the other nanotubes formed by α-amino acid residues,[39,40] the longer tubular systems outlined here are also expected to be biocompatible.

Theoretical Basis

Nomenclature. To systematically explore structural and energetic features of parallel sheets formed by β-peptides, six different models were constructed and studied: 2a, 2b, 2c, 2d, 3d, and 4d (Figure 2). For simplicity, all models are composed of the simplest achiral β-amino acid residue (β-Ala or homoGly) (Figure 1A). To provide relevant conformational data, both the N-and the C-termini of the peptide models were protected by an acetyl and an *N*-methylamine group, respectively, forming the $[CH_3CO-(\beta\text{-Ala})_k-NHCH_3]_l$ type model system. For describing the torsional angles of these β-peptides, the IUPAC-IUB recommendations of *gauche plus* (*g*+), *anti* (*a*), and *gauche minus* (*g*−) descriptors were applied. The noncovalently attached structures investigated in the present paper either can adopt a flattened reference (R^l) structure or can be rolled up into different nanotubes (T^l_{i+1}, T^l_{i+2}, T^l_{i+3}).

(38) Lehn, J.-M. *Supramolecular Chemistry: concepts and perspectives; a personal account*; VCH Verlagsgesellschaft mbH: Weinheim, 1995.
(39) Clark, T. D.; Buehler, L. K.; Ghadiri, M. R. *Journal of the American Chemical Society* **1998**, *120*, 651−656.
(40) Ghadiri, M. R.; Granja, J. R.; Buehler, L. K. *Nature* **1994**, *369*, 301−304.
(41) Hong, R.; Emrick, T.; Rotello, V. M. *Journal of the American Chemical Society* **2004**, *126*, 13572−13573.
(42) Gao, H. J.; Kong, Y. *Annual Review of Materials Research* **2004**, *34*, 123−150.
(43) Sazonova, V.; Yaish, Y.; Ustunel, H.; Roundy, D.; Arias, T. A.; McEuen, P. L. *Nature* **2004**, *431*, 284−287.
(44) Zhang, S. G. *Nature Biotechnology* **2003**, *21*, 1171−1178.
(45) Martin, C. R.; Kohli, P. *Nature Reviews Drug Discovery* **2003**, *2*, 29−37.
(46) Djalali, R.; Samson, J.; Matsui, H. *Journal of the American Chemical Society* **2004**, *126*, 7935−7939.
(47) Banerjee, I. A.; Yu, L. T.; Matsui, H. *Proceedings of the National Academy of Sciences of the United States of America* **2003**, *100*, 14678−14682.
(48) Hamada, N.; Sawada, S.; Oshiyama, A. *Physical Review Letters* **1992**, *68*, 1579−1581.
(49) Asthagiri, D.; Bashford, D. *Biophysical Journal* **2002**, *82*, 1176−1189.
(50) Frackenpohl, J.; Arvidsson, P. I.; Schreiber, J. V.; Seebach, D. *ChemBioChem* **2001**, *2*, 445−455.
(51) Hintermann, T.; Seebach, D. *Chimia* **1997**, *51*, 244−247.
(52) Seebach, D.; Albert, M.; Arvidsson, P. I.; Rueping, M.; Schreiber, J. V. *Chimia* **2001**, *55*, 345−353.
(53) Seebach, D.; Abele, S.; Gademann, K.; Guichard, G.; Hintermann, T.; Jaun, B.; Matthews, J. L.; Schreiber, J. V. *Helvetica Chimica Acta* **1998**, *81*, 932−982.
(54) Gellman, S. H. *Abstracts of Papers of the American Chemical Society* **1999**, *217*, U160−U160.
(55) Porter, E. A.; Wang, X. F.; Schmitt, M. A.; Gellman, S. H. *Organic Letters* **2002**, *4*, 3317−3319.
(56) Appella, D. H.; Christianson, L. A.; Klein, D. A.; Powell, D. R.; Huang, X. L.; Barchi, J. J.; Gellman, S. H. *Nature* **1997**, *387*, 381−384.
(57) Porter, E. A.; Weisblum, B.; Gellman, S. H. *Journal of the American Chemical Society* **2002**, *124*, 7324−7330.

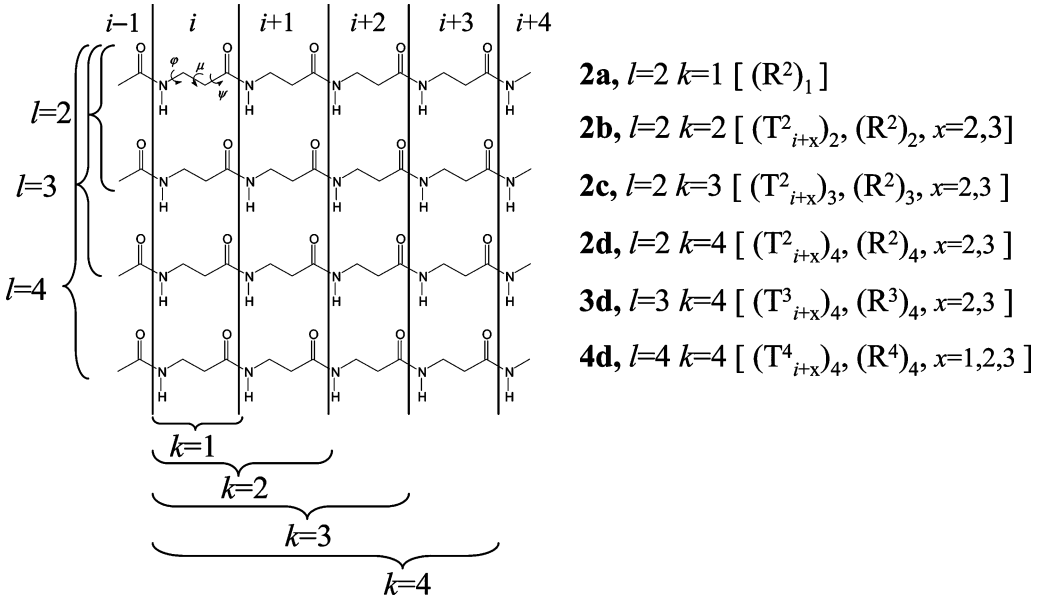

Figure 2. Schematic model and "nomenclature" of parallel sheet assemblies of β-peptides having 2 to 4 strands, where each individual strand could have 1 to 4 β-amino acid residues ($[CH_3CO-(\beta\text{-Ala})_k-NHCH_3]_l$ $1 \le k \le 4$ and $2 \le l \le 4$). The letter "*k*" indicates the total number of amino acid residues within the peptide chain, with "*i*" pointing to a relative sequential position and "*l*" showing the number of strands within the model system. On the right, the nomenclature (based on "*l*" and "*k*") describing the packing and structure of the models is shown.

Table 1. Levels of Theories Applied for the Structure and Stability Analysis of Parallel Sheet Assemblies of β-Peptides

method[a]	level of theory
mI	RHF/3-21G
mI/B	RHF/3-21G (BSSE)
mII	RHF/6-311++G(d,p)
mII/B	RHF/6-311++G(d,p) (BSSE)
mIII	B3LYP/6-31G(d)
mIII/B	B3LYP/6-31G(d) (BSSE)
mIV	B3LYP/6-311++G(d,p)
mIV/B	B3LYP/6-311++G(d,p) (BSSE)
mV	B3LYP/6-31G(d)//RHF/3-21G
mV/B	B3LYP/6-31G(d)//RHF/3-21G (BSSE)
mVI	B3LYP/6-311++G(d,p)//RHF/3-21G
mVI/B	B3LYP/6-311++G(d,p)//RHF/3-21G (BSSE)
mVII	B3LYP/6-311++G(d,p)//B3LYP/6-31G(d)
mVII/B	B3LYP/6-311++G(d,p)//B3LYP/6-31G(d) (BSSE)

[a] Model 2a was computed at every level of theory. However, larger structures (i.e., 2b, 2c, 2d, 3d, 4d) were studied only at mI, mIII, mVI, and mVII levels of theory.

Note that "R" stands for the reference, flattened or extended-like structure analogous to multiple stranded β-pleated sheets formed by α-peptides in proteins. The designation "T" represents any tubular system. The subscripts, $i + 1$, $i + 2$, $i + 3$, etc. characterize the pattern of hydrogen bonds operative between the first and the last strands "closing" the nanotube superstructure. All the other H-bonds within the model are of the {*i* to $(i + 1)$} type. Finally, subscript "*l*" denotes the number of β-strands in the nanotube, and *k* indicates the number of amino acid residues within a single strand. Therefore, the following shorthand notation has evolved: $(R^l)_k$, $(T^l_{i+1})_k$, $(T^l_{i+2})_k$, $(T^l_{i+3})_k$, etc. (Figure 3).

Computational Details. All computations were carried out using the Gaussian 03 software package.[58] To estimate the magnitude of *B*asis *S*et *S*uperposition *E*rror (BSSE), geometry optimization of the $[CH_3-CO-\beta\text{-Ala}-NHCH_3]_2$ model (2a) using a structure composed of two S_{PM} monomers[25] was carried out at all applied levels of theories (Table 1 and Supporting Information STable 1). Geometry optimizations of the 2b, 2c, 2d, 3d, and 4d models were completed at the RHF/3-21G (mI) and the B3LYP/6-31G(d) (mIII) levels of theory (Figure 2 and STable 2). All fully optimized supramolecular conformers ($(R^l)_k$, $(T^l_{i+1})_k$, $(T^l_{i+2})_k$, $(T^l_{i+3})_k$, etc.) were subjected to single-point energy calculations carried out at the B3LYP/6-311++G(d,p)//RHF/3-21G (mVI) and B3LYP/6-311++G(d,p)//B3LYP/6-31G(d) (mVII) levels of theory (Table 2).

As previously described,[25] the most stable backbone-fold of a single β-peptide composed of four amino acid residues in a vacuum is the $(Z6_P)_4$, a zigzag, or elongated helical fold. Therefore, the $(Z6_P)_4$ type conformer of $CH_3CO-(\beta\text{-Ala})_4-NHCH_3$ was optimized at the mI and mIII levels of theory, followed by DFT single-point energy calculations carried out at both the mVI and mVII levels of theory (Tables 1 and 3). This structure was used as the reference to estimate the energy gains during self-assembly of the single-stranded β-peptides.

The stability of all the alternative tertiary structures $\{(R^l)_4$, $(T^l_{i+1})_4$, $(T^l_{i+2})_4$, $(T^l_{i+3})_4\}$ of the different peptide models (e.g., two-stranded, 2d, three-stranded, 3d, four-stranded, 4d, etc.) were compared by using two scales: a *per* unit (i.e., *per* residue) and a *per* hydrogen bond stability scale (Table 3).

For more details on computation see Supporting Information.

Results and Discussion

Precision and Accuracy. To estimate the effect of basis set and electron correlation on structure and stability of the noncovalently attached subunits and to find a suitable method for larger nanosystems, the smallest model, 2a, has been investigated at various levels of theory (STable 1). Analysis of the geometrical properties as a function of the applied level of theory shows that optimizations on smaller DFT/DZP type basis sets provide adequate structures, thus B3LYP/6-31G(d) level of theory is used for optimizations throughout this paper, unless mentioned otherwise.

The magnitude of BSSE was also estimated at different levels of theory, and it was found that for a TZP type basis set (B3LYP/6-311++G(d,p) or mVII) the magnitude of BSSE is as small as ~0.5 kcal mol^{-1}; therefore mVII is used throughout this paper for stability analysis of larger nanosystems.

(58) Frisch, M. J.; et al. Gaussian, Inc.: Wallingford, CT, 2004.

Table 2. Relative Stability and H-Bond Parameters of the Different Supramolecular Complexes of Multiple Stranded Parallel Sheet Models of $[CH_3CO-(\beta\text{-Ala})_k-NHCH_3]_l$ ($2 \le k \le 4$ and $2 \le l \le 4$)

model	structure[a]	H-bonds[b]	ΔE_{mVII}[c]	$d_{O\cdots H}$[Å][f]	$d_{O\cdots N}$[Å][f]	α_{O-H-N}[d,f]
2b	$(R^2)_2$	$3 = 3$	0.0	2.06 (0.02)	3.06 (0.03)	172.55 (6.30)
	$(T^2_{i+2})_2$	$\mathbf{2} + 2 = 4$	−7.5	2.05 (0.06)	3.01 (0.08)	162.47 (18.25)
	$(T^2_{i+3})_2$	$\mathbf{1} + 3 = 4$	−5.0	2.00 (0.21)	3.04 (0.13)	164.72 (14.11)
2c	$(R^2)_3$	$4 = 4$	0.0	2.04 (0.10)	3.05 (0.08)	173.41 (7.40)
	$(T^2_{i+2})_3$	$\mathbf{3} + 2 = 5$	−10.1	2.07 (0.04)	3.03 (0.07)	161.52 (13.93)
	$(T^2_{i+3})_3$	$\mathbf{2} + 4 = 6$	−11.2	2.07 (0.04)	3.06 (0.04)	164.22 (6.75)
2d	$(R^2)_4$	$5 = 5$	0.0	2.10[e] (0.00)	3.09 (0.02)	164.18 (5.86)
	$(T^2_{i+2})_4$	$\mathbf{2} + 3 = 5$	−8.8	2.32 (0.38)	3.14 (0.16)	143.19 (24.18)
	$(T^2_{i+3})_4$	$\mathbf{3} + 5 = 8$	−16.3	2.06 (0.11)	3.04 (0.09)	162.33 (7.85)
3d	$(R^3)_4$	$5 + 5 = 10$	0.0	2.02 (0.04)	3.03 (0.04)	172.10 (2.67)
	$(T^3_{i+2})_4$	$\mathbf{4} + 5 + 5 = 14$	−22.7	2.08 (0.06)	2.99 (0.03)	149.79 (8.95)
	$(T^3_{i+3})_4$	$\mathbf{3} + 5 + 5 = 13$	−32.2	2.00 (0.04)	2.98 (0.05)	163.58 (4.72)
4d	$(R^4)_4$	$5 + 5 + 5 = 15$	0.0	1.99 (0.03)	3.00 (0.03)	172.99 (2.37)
	$(T^4_{i+1})_4$	$\mathbf{5} + 5 + 5 + 5 = 20$	−27.5	2.05 (0.06)	2.98 (0.04)	150.73 (6.34)
	$(T^4_{i+2})_4$	$\mathbf{4} + 5 + 5 + 5 = 19$	−43.6	1.96 (0.03)	2.93 (0.02)	157.63 (5.75)
	$(T^4_{i+3})_4$	$\mathbf{3} + 5 + 5 + 5 = 18$	−46.1	1.95 (0.04)	2.95 (0.04)	166.63 (3.45)

[a] For more details on nomenclature, see Theoretical Basis. [b] Total number of $\{i \rightarrow (i+1)\}$-type hydrogen bonds between β-strands plus the number of hydrgoen bonds closing the nanotubes in bold (see Figure 4). [c] All relative energies are in kcal mol^{-1} (mVII: B3LYP/6-311++G(d,p)//B3LYP/6-31G(d)). [d] Angle in degrees. [e] Hydrogen bonds constrained to 2.1 Å. [f] Average hydrogen bond distances (or H-bond angles) with standard deviations in parentheses.

Table 3. Stability of the Different Tertiary Structures Composed of Two-, Three-, and Four-Stranded Tetra-β-peptides (2d, 3d, and 4d, respectively). All Energies Are Relative to $(Z6_P)_4$, a Single-Stranded Tetra-β-peptide, $CH_3CO-(\beta\text{-Ala})_4-NHCH_3$

model	structure[a]	ΔE_{mVI}[b]	ΔE_{mVII}	units[c]	ΔE_{mVII}/ unit	H-bonds	ΔE_{mVII}/ hydrogen bond
2d	$2^*(Z6_P)_4$	0.0	0.0	8	0.0		
	$(R^2)_4$	13.9	12.8		1.6	5	2.6
	$(T^2_{i+2})_4$	5.9	4.1		0.5	5	0.8
	$(T^2_{i+3})_4$	−2.3	−3.4		−0.4	8	−0.4
3d	$3^*(Z6_P)_4$	0.0	0.0	12	0.0		
	$(R^3)_4$	3.3	−0.1		0.0	10	0.0
	$(T^3_{i+2})_4$	−20.8	−22.8		−1.9	14	−1.6
	$(T^3_{i+3})_4$	−28.5	−32.3		−2.7	13	−2.5
4d	$4^*(Z6_P)_4$	0.0	0.0	16	0.0		
	$(R^4)_4$	−12.0	−17.5		−1.1	15	−1.2
	$(T^4_{i+1})_4$	−38.6	−45.0		−2.8	20	−2.3
	$(T^4_{i+2})_4$	−54.8	−61.1		−3.8	19	−3.2
	$(T^4_{i+3})_4$	−58.9	−63.6		−4.0	18	−3.5

[a] For more details on nomenclature see Theoretical Basis. [b] Energies are in kcal mol^{-1} and relative to $(Z6_P)_4$ (mVI: B3LYP/6-311++G(d,p)//RHF/3-21G, mVII: B3LYP/6-311++G(d,p)//B3LYP/6-31G(d)). [c] Number of β-alanine residues (i.e., units).

For more details on precision and accuracy see Supporting Information.

Structure and Stability of the Four-Stranded Tetrapeptide Models. First, the structural and energetic properties of the longest tubular assemblies of 4d, $[CH_3CO-(\beta\text{-Ala})_4-NHCH_3]_4$, were described. This system consists of a total of four noncovalently attached β-strands, where each tetrapeptide has suitable N- and C-terminal protecting groups. For 4d, three different tubular conformers were optimized, $(T^4_{i+1})_4$, $(T^4_{i+2})_4$, and $(T^4_{i+3})_4$ with the reference structure $(R^4)_4$ (see Theoretical Basis for the nomenclature of abbreviations) (Figure 3A and B). The three supramolecular complexes with a tubular shape have different hydrogen bond pairing patterns between the "first" and the "last" β-strands. As long as $(T^4_{i+1})_4$ has an $\{i$ to $(i+1)\}$, $(T^4_{i+2})_4$ has an $\{i$ to $(i+2)\}$ and $(T^4_{i+3})_4$ incorporates an $\{i$ to $(i+3)\}$ pairing (Figure 4). Adoption of the tubular shape for 4d is "spontaneous"; thus, flattening of the reference conformer $(R^4)_4$ is achieved by suitable torsional constraint(s) [see Theoretical Basis and Supporting Information].

The comprehensive structural analysis of $(R^4)_4$, $(T^4_{i+1})_4$, $(T^4_{i+2})_4$, and $(T^4_{i+3})_4$ revealed that their component β-strands have similar conformational properties. These strands are composed of highly similar subunit structures with backbone torsions as follows: $\varphi \approx [g^-]$, $\mu \approx [a]$, and $\psi \approx [a]$ (Figure 1 and STable 2) also labeled as S_{PM} in a preceding paper.[25] Even $(R^4)_4$, which has a flattened and therefore very different tertiary structure, is composed of conformational building units of a very similar nature. For example, variations of torsional angles around $\varphi \approx [g^-]$, $\mu \approx [a]$, and $\psi \approx [a]$ in both $(T^4_{i+2})_4$ and $(T^4_{i+3})_4$ are as low as 7.7° and 11.0°, respectively, at the mIII level of theory. In contrast, $(T^4_{i+1})_4$ exhibits larger torsional angle variations, signaling the presence of less uniform S_{PM}-type conformational subunits. This may indicate that a $(T^4_{i+1})_4$ tubular system is less relaxed when it displays more conformational diversity. Similar to $(T^4_{i+1})_4$, the reference structure $(R^4)_4$ also presents an increase in local backbone conformational variability (STable 2).

In summary, some local conformational fluctuations of the component subunits were observed in both $(T^4_{i+1})_4$ and $(R^4)_4$, but these variations have no considerable effect on the overall fold of tertiary structures. Unlike local structural properties, stability data of these nanotubes are very different (Table 2). Relative to the flattened structure $(R^4)_4$, rolling into any tubular structure is always preferred. The energy difference between the flattened $(R^4)_4$ reference superstructure and that of the $(T^4_{i+1})_4$ is −27.5 kcal mol^{-1} at the mVII level of theory ($\Delta E_{(R4)4 \rightarrow (T4i+1)4} = -27.5$ kcal mol^{-1}) (Table 2). Note that the folding of the latter structure, $(T^4_{i+1})_4$, from $(R^4)_4$ is accompanied through the formation of an additional five $\{i$ to $(i+1)\}$-type hydrogen bonds. As long as $(R^4)_4$ consists of 15 hydrogen bonds, a total of 20 can be assigned in $(T^4_{i+1})_4$. When H-bond parameters were analyzed for $(R^4)_4$, we found that the average O···H distance ($d_{O\cdots H}$) is 1.99 ± 0.03 Å. For the same system, the O···N bond length ($d_{O\cdots N}$) averages 3.00 ± 0.03 Å, accompanied by an H-bond angle (α_{O-H-N}) of 173.0 ± 2.37°. Although five additional H-bonds appear in $(T^4_{i+1})_4$ compared

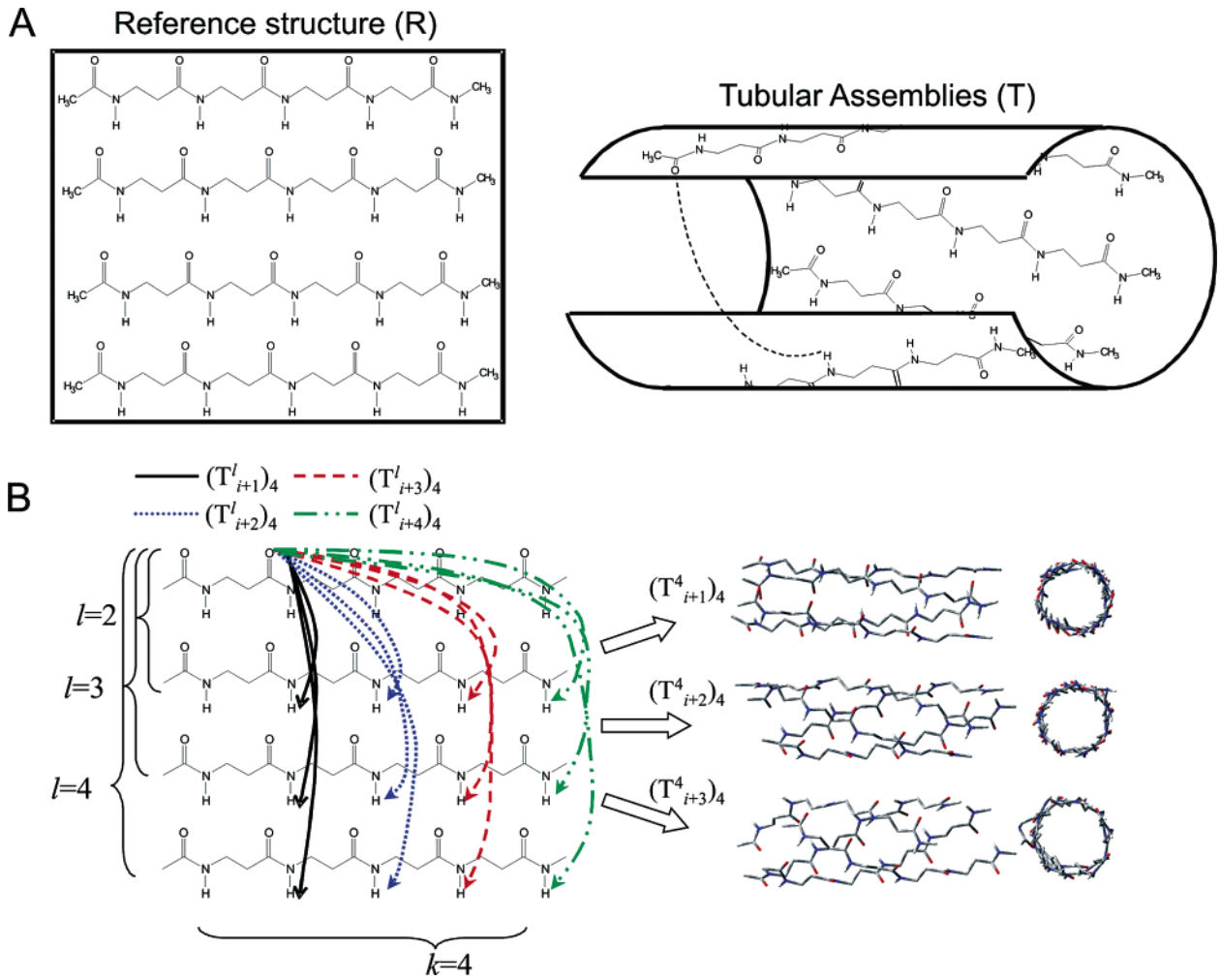

Figure 3. (A) Schematic view of the extended reference structure (R) and the rolling up of the tubular multistranded assemblies (T). (B) Formation of the different hydrogen bond networks between the first and the "last" (l th) strands of the "tubular sheet assemblies" of [$CH_3CO-(\beta$-Ala$)_4-$NHMe$]_l$ ($2 \le l \le 4$). Both side and top views of four-stranded tubular structures, $(T^4_{i+1})_4$, $(T^4_{i+2})_4$, and $(T^4_{i+3})_4$, are shown.

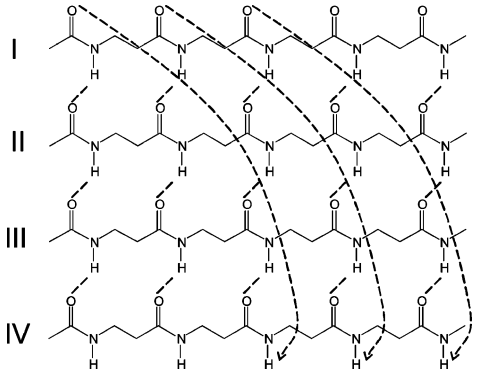

Figure 4. A total of 18 hydrogen bonds (5 + 5 + 5 + 3) are effective in $(T^4_{i+3})_4$ as marked by dashed lines. Besides the "conventional" $\{i \rightarrow (i+1)\}$-type hydrogen bonds, a total of 15, those 3 marked by dashed arrows connect the first (I) and the fourth (IV) β-strands and are of $\{i \rightarrow (i+3)\}$-type.

to $(R^4)_4$, they all are "weakened". In fact, all 20 hydrogen bonds of $(T^4_{i+1})_4$ are longer (e.g., $d_{O\cdots H}$ longer by ~0.06 Å) than those in the reference structure.

Stability differences are even larger for $(T^4_{i+2})_4$ and $(T^4_{i+3})_4$ tubular superstructures at −43.6 and −46.1 kcal mol^{-1}, respectively (Table 2). One may wonder about the origin of the increased stability of both $(T^4_{i+2})_4$ and $(T^4_{i+3})_4$, since fewer H-bonds are present than those in $(T^4_{i+1})_4$. There are a total of 19 H-bonds in $(T^4_{i+2})_4$ and 18 in $(T^4_{i+3})_4$. The apparent contradiction of "fewer H-bonds with higher stability" is partially resolved by the analysis of their H-bond parameters. Although only 19 hydrogen bonds in $(T^4_{i+2})_4$ (15 $\{i \rightarrow (i+1)\}$ and 4 $\{i \rightarrow (i+2)\}$ are present, the H-bond parameters are more favorable than they are in $(T^4_{i+1})_4$. The O···H distances are shortened by ~0.09 Å ($d_{H\cdots O}$ = 1.96 Å) with a deviation of ~0.03 Å) (Table 2). In addition, H-bonds are less tilted in $(T^4_{i+2})_4$ than they are in $(T^4_{i+1})_4$, which is a more favorable scenario ($\alpha_{O-H-N} = 157.63 \pm 5.75°$) and further increases the overall stability of the supramolecule. The same observation holds for $(T^4_{i+3})_4$. In the latter structure, a total of 18 intramolecular hydrogen bonds can be assigned with H-bond parameters even more favorable than they are in $(T^4_{i+2})_4$. The O···H distances are further shortened by ~0.01 Å ($d_{H\cdots O} = 1.95 \pm 0.04$ Å), with less tilted ($\alpha_{O-H-N} = 166.63°$) H-bond angles. Indeed, the improved H-bond parameters result in higher stability ($\Delta\Delta E_{mVII} = 2.5$ kcal mol^{-1}) (Table 2) despite a reduction in the total number of H-bonds in $(T^4_{i+3})_4$ compared to $(T^4_{i+2})_4$.

Relative to the reference structure $(R^4)_4$, the increased stability of the tubular assemblies also originates from the improved local conformational properties as well as the bending or rolling of

Chart 1. Nanotube Structures of $[CH_3CO-(\beta\text{-Ala})_4-NHCH_3]_l$ ($2 \leqslant l \leqslant 4$) Tetra-$\beta$-peptides[a]

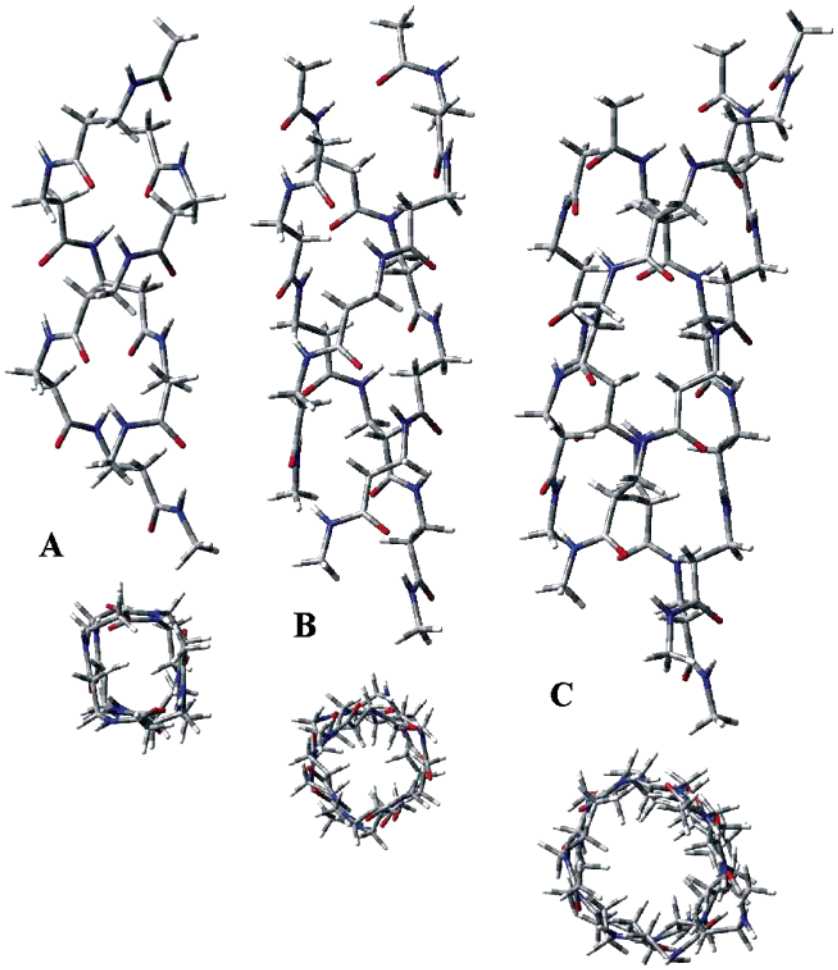

[a] (A) $(T^2_{i+3})_4$ structure of 2d; (B) $(T^3_{i+3})_4$ structure of 3d; and (C) $(T^4_{i+3})_4$ structure of 4d.

Chart 2.[a]

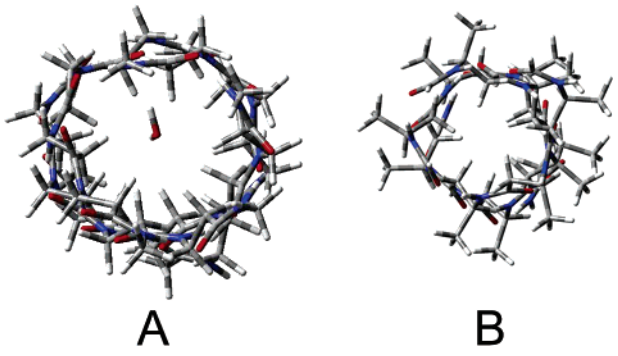

[a] (A) The $(T^4_{i+3})_4$ tubular structure of 4d, incorporating a water molecule. (B) The $(T^3_{i+3})_4$ nanotube structure of $[CH_3CO-(\beta\text{-Abu})_4-NHCH_3]_3$ with $\beta^3(S)$ chirality. All side-chain methyl groups are equatorially positioned and, thus, pointing outward from the surface of the nanotube.

the flattened system into a tubular structure, which is accompanied by an increased number of H-bonds. Furthermore, increased stability of the tubular systems is enforced not only by maximizing the total number of H-bonds holding the system together but also by forming H-bonds with improved geometrical parameters. One may wonder whether shorter and tighter tubular models have a similar strategy of self-stabilization.

Structure and Stability of the Two- and Three-Stranded Tetrapeptide Models. The comprehensive analysis of the three-stranded systems (3d) show great similarity to what is observed for four-stranded models (4d). As discussed for four-stranded systems, the total number of hydrogen bonds is not necessarily the ultimate parameter to be maximized for gaining extra stability. Improving both hydrogen bond parameters $d_{O\cdots HN}$ and $d_{O\cdots N}$ also increases the stability of the tertiary structure. Although $(T^3_{i+3})_4$ contains fewer hydrogen bonds than $(T^3_{i+2})_4$ by 1, 13, and 14, respectively, the stability of the former supramolecular system is far better ($\Delta E_{(T^3_{i+3})_4} = -32.2$ kcal mol^{-1}) than that of $(T^3_{i+2})_4$: $\Delta E_{(T^3_{i+2})_4} = -22.7$ kcal mol^{-1} (Table 2). Indeed, the H-bond parameters are more favorable in $(T^3_{i+3})_4$ than they are in $(T^3_{i+2})_4$: O···H distances are shortened by 0.08 ± 0.04 Å ($d_{H\cdots O} = 2.00$ Å). The improved distances occur in conjunction with more favorable hydrogen bond angle parameters ($\alpha_{O-H-N} = 163.58 \pm 4.72°$).

Two-stranded models composed of a total of 2, 3, and 4 amino acid residues per peptide strand (2b, 2c, and 2d) were also studied. Due to steric hindrances, two- and three-stranded molecular systems were too tight to form hydrogen-bonded nanotubes, with the "first" and the "last" β-strands interconnected by $\{i \rightarrow (i+1)\}$-type hydrogen bonds resulting in a $(T^2_{i+1})_k$ structure. Therefore, the stability and structure of $(R^2)_k$, $(T^2_{i+2})_k$, and $(T^2_{i+3})_k$ were compared. Conformational analysis revealed that the local conformational properties of the three models are quite similar to those composed of three and four β-strands (STable 2), although with a slightly more pronounced

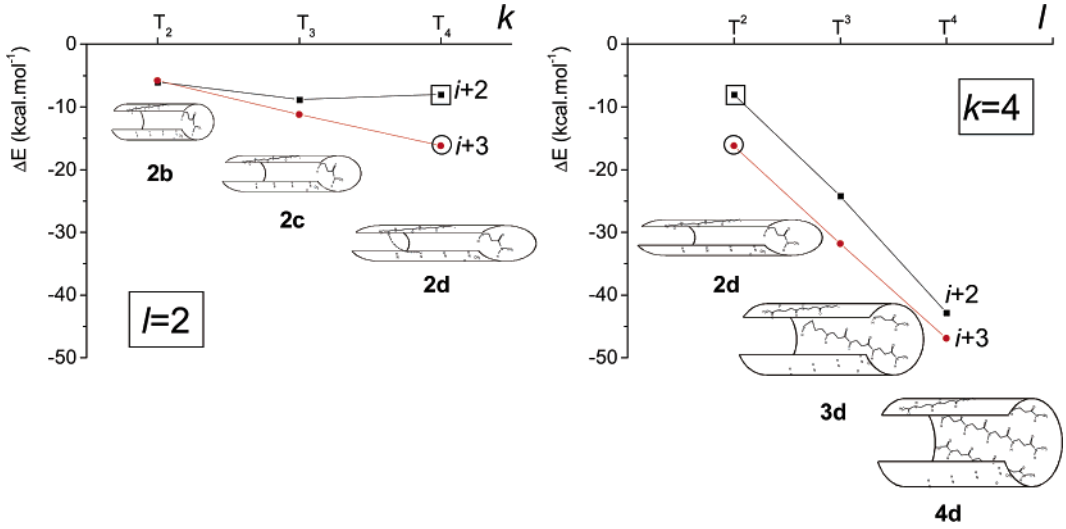

Figure 5. Variation of nanotube stabilization energies with increasing k and l for $[CH_3CO-(\beta\text{-Ala})_k-NHCH_3]_l$. The type of hydrogen bond pairing in the tube-closing network is labeled as $(i + 2)$ and $(i + 3)$. The two open squares as well as the two open circles denote duplicate data points.

conformational diversity for $(R^2)_k$-type structures than for those of tubular nature. Analysis of the energetic properties of two-stranded systems showed that the tubular structures $(T^2_{i+2})_k$ and $(T^2_{i+3})_k$ were once again more stable than the flattened reference structures, $(R^2)_k$ $(2 \le k \le 4)$ (Table 2). Considering the shortest model containing two β-Ala residues per strand, the tubular structure $(T^2_{i+2})_2$ has a relative stability difference of -7.5 kcal mol^{-1} ($\Delta E_{(R^2)_2 \rightarrow (T^2_{i+2})_2}$) at the mVII level of theory (2b). The same holds for $(T^2_{i+3})_2$; namely $\Delta E_{(R^2)_2 \rightarrow (T^2_{i+3})_2} = -5.0$ kcal mol^{-1}. Thus, even the shortest and the tightest tubular systems are more stable than their parent and fully flattened reference structure.

Increasing the number of amino acid residues per strand from 2 to 3 and from 3 to 4 also increases the stability of the tubular systems. As long as $(T^2_{i+3})_2$ is more stable than its reference structure $(R^2)_2$ by -5.0 kcal mol^{-1} ($\Delta E_{(R^2)_2 \rightarrow (T^2_{i+3})_2} = -5.0$ kcal mol^{-1}), the stability of $(T^2_{i+3})_3$ is even greater (-11.2 kcal mol^{-1}). This difference further increases for $(T^2_{i+3})_4$: $\Delta E_{(R^2)_4 \rightarrow (T2^2_{i+3})_4} = -16.3$ kcal mol^{-1} at the mVII level of theory (Table 2). The enhanced stability correlates with the increasing number of $\{i \rightarrow (i + 3)\}$-type hydrogen bonds, present in all of the tubular structures, $(T^2_{i+3})_2$, $(T^2_{i+3})_3$, $(T^2_{i+3})_4$, compared to their parent reference systems $(R^2)_2$, $(R^2)_3$, and $(R^2)_4$ (Table 2). Thus, the -5.0 kcal mol^{-1}, -11.2 kcal mol^{-1}, and -16.3 kcal mol^{-1} stabilization energies are proportional with the one, two, and three extra hydrogen bonds. The $\sim$5.5 kcal mol^{-1} increase in stability per hydrogen bond is in agreement with previous data (Table 2).[59−60]

In conclusion, all tubular systems are more stable than their parent reference structures. This is achieved by increasing the total number of hydrogen bonds and improving the hydrogen bond parameters holding the tertiary structures together and the conformational parameters of the monomeric units.

Structure and Stability of Models Composed of Different Numbers of Strands but with the Same Length of Component Chains. To explore the tubular assembling potential of the model systems composed of two, three, and four β-strands, three tetra-β-peptides (2d, 3d, and 4d) were analyzed (STable 2, Table 2, Table 3, and Chart 1). As discussed above, the two- and three-stranded tubular structures with $\{i \rightarrow (i + 1)\}$-type hydrogen bonds, $(T^2_{i+1})_4$, $(T^3_{i+1})_4$, cannot be optimized, due primarily to steric interactions. Thus, the present comparison focuses on stability analyses of the $(R^l)_4$, $(T^l_{i+2})_4$, and $(T^l_{i+3})_4$ $(2 \le l \le 4)$ tertiary structures, with a four-residue long isolated polypeptide chain having an elongated helical or zigzag-type, $(Z6_P)_4$, secondary structure (Table 3).

When comparing "aggregation" or tertiary structure formation properties of the model systems, it is clear that although the $(Z6_P)_4$ structure contains hydrogen bonds, its noninteractive assembly can be more or less stable compared to the appropriate extended structure, $(R^l)_4$. Therefore, reference structures with relative energy 0.0 kcal mol^{-1} are the combination of two, three, or four of the noninteracting $(Z6_P)_4$ conformers, depending on the system to be analyzed (Table 3). Note that for two- and three-stranded systems, the appropriate extended structures $(R^2)_4$ and $(R^3)_4$ are less stable than the noninteracting groupings of two or three $(Z6_P)_4$ conformers: $\Delta E_{2*(Z6_P)_4 \rightarrow (R^2)_4} = +12.8$ kcal mol^{-1} and $\Delta E_{3*(Z6_P)_4 \rightarrow (R^3)_4} = -0.1$ kcal mol^{-1}, respectively (Table 3). However, the four-stranded extended system $(R^4)_4$ is more stable than the noninteracting ensemble of four $(Z6_P)_4$ helices: $\Delta E_{4*(Z6_P)_4 \rightarrow (R^4)_4} = -17.5$ kcal mol^{-1}.

By comparing all 9 interacting and all 3 noninteracting structural complexes (Table 3) regardless of the type of hydrogen bonds, the four-stranded tubular structures $(T^4)_4$ are the most stable assemblies. Although three-stranded tubular systems $(T^3)_4$ are less stable than four-stranded ones, they are more stable than the two-stranded complexes $(T^2)_4$. Thus, widening the tube seems to stabilize tertiary structure.

When comparing tubular systems composed of four, three, or two β-strands and having the same type of hydrogen bonding pattern (e.g., $\{i \rightarrow (i + 3)\}$) interconnecting the "first" and the "last" strands, the large stability difference per amino acid residue is remarkable for the four- and the three-stranded

(59) Perczel, A.; Hudaky, P.; Fuzery, A. K.; Csizmadia, I. G. *Journal of Computational Chemistry* **2004**, *25*, 1084−1100.
(60) Abbreviations: β-Ala, 3-amino-propanoic acid; β-homoglycine, β-HGly; β-Abu, 3-amino-butanoic acid; β-homoalanine, (3*S*)-β-(HAla); PNA, peptide nucleic acid; *trans*-2-ACHC, *trans*-2-aminocyclohexane carboxylic acid; *trans-cis*-ACPC, *trans-cis*-aminocyclopentane carboxylic acid; Pro-DADME, prolyl-[1,2-diamino-1,1-dimethyl ethane]; DZP, double-ζ basis plus polarization functions; TZP, triple-ζ basis plus polarization functions; U4 $\equiv S_{PM} \equiv g+[a]a$ conformer.

tubes: $\Delta E_{(Z6p)_4\rightarrow(T^4_{i+3})_4} = -4.0$ kcal mol^{-1}, $\Delta E_{(Z6p)_4\rightarrow(T^3_{i+3})_4} = -2.7$ kcal mol^{-1}, and $\Delta E_{(Z6p)_4\rightarrow(T^2_{i+3})_4} = -0.4$ kcal mol^{-1}, respectively, at the mVII level of theory. Stability differences correlate with the total number of hydrogen bonds present in the assembly of superstructures (18, 13, and 8, respectively). Stability also increases with the widening of the tubular system, which brings the hydrogen bond parameters closer to their ideal values. For example, the average O···H distances of the narrower $(T^2_{i+3})_4$ is reduced from 2.06 Å to 2.00 Å in the wider $(T^3_{i+3})_4$. In the widest $(T^4_{i+3})_4$ structure, the average hydrogen bond distance is even shorter at 1.95 Å (Table 2). Thus, shortening hydrogen bonds are associated with an increase in stability. The same observation holds for tubular systems equipped with $\{i \rightarrow (i + 2)\}$-type hydrogen bonds connecting the "first" and the "last" strands. In conclusion, widening the tubular systems simultaneously increases the number of hydrogen bonds and improves the structural parameters of the monomeric units (i.e., the backbone torsional angles of the monomeric units in the tubular structures are less shifted from the ideal S_{PM} values than those of the constrained reference structures), which has the overall effect of increasing the stability of the molecular complex. In addressing the question of structure and stability, it should be pointed out the large values of stabilization mentioned above (-63.6 kcal mol^{-1} or -32.3 kcal mol^{-1}, Table 3) are not that excessive when divided by the number of peptide units (see ΔE_{mVII}/unit, Table 3) or the number of hydrogen bonds involved (see ΔE_{mVII}/hydrogen bond, Table 3). These two values were found to be -4.0 kcal mol^{-1} and -3.5 kcal mol^{-1}, respectively, for $\Delta E_{mVII} = -63.6$ kcal mol^{-1}.

Based on the tendency observed in the case of three- and four-stranded systems we are quite sure that five- and six-stranded systems are also stable, or perhaps even more stable than the four-stranded ones. This prediction is even more likely if one considers that more shifted hydrogen bond patterns (i.e., $i + 4$ or $i + 5$) could also appear, which could further relax a multiple stranded system. Nevertheless the stability of these large assemblies depends on many parameters; thus their relative stability compared to the three- or four-stranded systems is unpredictable at the present time. Unfortunately, geometry optimization of 25−30 or more β-amino acids in five to six different molecules at the B3LYP/6-31G(d) level of theory would require an insurmountable amount of CPU time and possibly would not really provide new concepts.

Note that although these tubular structures of β-peptides are quite similar to β-barrels observed in natural proteins,[11−14] only two β-peptides are already enough to form a tubular structure, and four strands form quite stable tubes, whereas β-barrels are usually formed from at least 10 α-peptide strands. This phenomenon is apparently due to the local conformational flexibility of the β-peptides.

Finally, the entropy of folding needs to be considered. For example, the following has been computed previously for $g + aa$ (U4 ≡ S_{PM}) at the B3LYP/6-311++G(d,p) level of theory for conformational folding:[26]

$$\Delta G = \Delta H - T\Delta S = -2.07 - 0.64 = -2.71 \text{ kcal mol}^{-1}$$

Clearly, the entropy change in terms of $T\Delta S$ is significant, but ΔH still dominates ΔG. It is therefore reasonable to assume that the -63.6 kcal mol^{-1} value generated above would need to be coupled with a considerably smaller $T\Delta S$ value within the calculation of ΔG. Consequently, the relative energies are anticipated to illustrate the energetic background of the self-assembled tubular structures in the thermodynamic sense fairly well.

Such a conclusion may be accepted until it becomes feasible to reliably compute entropy contributions for relatively large nanostructures.

Applicability as Nanotubes. In contrast to earlier peptide nanotubes that have cyclic peptides as building blocks,[39,40] these tubes are formed from noncyclic, i.e., linear strands. Nevertheless, to form multipurpose and useful nanotubes, these structures must meet criteria in addition to energetic preference. One might be the interior diameter of the tube, which would need to be large enough to incorporate smaller molecules, atoms, or ions. The approximate interior diameters of the 2d and 3d tubes are ∼4 Å and ∼5 Å, respectively, which were found to be too tight for small molecules to pass through. In the case of 4d, the tube has a ∼6 Å diameter, which is large enough for a small molecule like water to be coordinated through (Chart 2A).

To fulfill a variety of purposes, the feasibility of different side chains could be assessed. As a preliminary study, the four-stranded $(T^3_{i+3})_4$ structure of $[CH_3CO-(\beta\text{-Abu})_4-NHCH_3]_3$, which has methyl side chains on each β^3-atom with an *S* absolute configuration (Chart 2B), was optimized at the mI level of theory. According to this structure, all the methyl groups are equatorial and pointing outward from the surface of the tube. This feature shows that, even for a smaller model, the outer side chains do not have a significant structure modifying effect on these tubular structures. Note that the prochiral *S* hydrogen atoms of all the β^2-atoms point toward the inside center of the tube, which could, among other roles, coordinate small reactants. Nevertheless, the ∼6 Å diameter of the $(T^4_{i+3})_4$ is too small to apply inner side chains.

Although the four-stranded tube has an acceptable interior diameter for small molecules to penetrate, their behavior in solvent(s) needs to be explored. Solvation properties are mostly dependent on the type of side chains used. However, applying different solvation models, testing different side chains, and investigating the dynamic properties of these tubular systems are beyond the scope of the present study.

Conclusions

To characterize the sheet assembly properties of β-peptides, structural investigations of a set of model β-peptides $[CH_3CO-(\beta\text{-Ala})_k-NH-CH_3]_l$ ($2 \le k \le 4$, $1 \le l \le 4$) were performed at different levels of theory (Figure 2, STable 2). It was found that sheets of β-peptides have fundamentally different behaviors when compared to α-peptides (Figure 3). In contrast to the parallel β-sheet structure of α-peptides adopting an extended-like backbone conformation, two-, three-, and four-stranded β-peptide models fold into several types of tubular structures (Figures 3, 4, and Chart 1). In this study, four types of structures were investigated in detail: $(T^l_{i+1})_k$, $(T^l_{i+2})_k$, $(T^l_{i+3})_k$, and $(R^l)_k$ ($2 \le k \le 4$, $2 \le l \le 4$), where the last is used as a reference structure. $(T^l_{i+1})_k$, $(T^l_{i+2})_k$, and $(T^l_{i+3})_k$ are tubular structures, where $i + x$ refers to the hydrogen bonding pattern between the first and the last strand. Each structure has similar backbone torsional angles: $\varphi = [g^-]$, $\mu = [a]$, $\psi = [a]$ (STable 2). The energetic distribution of these tubular structures shows that they are preferred over the opened classical pleated sheet structures

$(R^l)_k$ (Tables 2 and 3). Of all investigated structures, the four-stranded $(T^4_{i+3})_4$ is the most stable, with a relative energy of -46.1 kcal mol^{-1} compared to $(R^4)_4$. A graphical illustration of the relative stabilities as functions of increasing k and l is shown in Figure 5.

To describe potential applications of these nanotubes with other special characteristics, further studies are needed. The interior diameter of the four-stranded $(T^4_{i+3})_4$ structure is approximately 6 Å, which is large enough to coordinate water molecules through (Chart 2A). Thus, to determine the stability as a function of the number of strands and to increase the interior diameter, five- and six-stranded tubes should be optimized as well; nevertheless current computational methods are not sophisticated enough to carry out such computations practically in a considerable amount of time. According to preliminary studies on the $(T^3_{i+3})_4$ structure, the orientation of the side chains appears ideal, since the β^3(S) side chains point toward the outer matrix, while the β^2(S) side chains point toward the vertical axis of the tube (Chart 2B). Thus, although the investigated simple β-Ala-containing model peptides do not form the theoretically observed nanostructures in solution, it seems possible to apply special side chains with appropriately chosen polarity that would interact with the outer solvent molecules and stabilize such a structure. In contrast to the above, other side chains would selectively coordinate small compounds inside the tube.

Formed from single-stranded peptides, these nanotubes are unique, since previous peptide nanotubes were assembled from cyclic peptides.[39,40]

In summary, based on reliable intermediate level theoretical calculations (B3LYP/6-31G(d), B3LYP/6-311++G(d,p)//B3LYP/6-31G(d)), the existence of supersecondary sheet structures of β-peptides (or nano-structures) was outlined. Although there are experimental evidences supporting the notion that such nanotubes can be formed from β-peptides, the present theoretical study demonstrates their intrinsic stability. With the careful selection of side chains and molecular environments, unique systems could be engineered in the future. These β-peptide tubes could then have diverse applications, since the orientation of the side chains is suitable to design various environments for the inner and outer surfaces. Future studies to characterize nanotubes equipped with different side chains are required, which will create models for forthcoming experimental studies. It is hoped that the present paper will stimulate experimental research in the field of nanostructure technology involving β-peptides.

Acknowledgment. This research was supported by grants from the Hungarian Scientific Research Foundation (OTKA T046994 and TS044730) and MediChemBats2. I.G.C. wishes to thank the Ministry of Education of Hungary for the award of a Szent-Györgyi Visiting Professorship. The authors also thank Suzanne Lau for assistance in preparing the manuscript.

Supporting Information Available: Computational Details, Precision and Accuracy, and Cartesian coordinates of 2d, 3d, and 4d, as well as complete ref 58. This material is available free of charge via the Internet at http://pubs.acs.org.

JA0585127